

Early Detection of Oak Wilt Disease in Quercus ssp.: A Hyperspectral Approach

**A term paper in partial fulfillment
for the requirements of ES6973**

Dr. Hongjie Xie

**Prepared by
Blake Weissling
PhD Student**

**University of Texas San Antonio
May 6, 2005**

Abstract

Initial work has begun on a long-term study of the application of spectroradiometric techniques to spectral discrimination of oak wilt disease in Quercus woodlands of central Texas. In situ hyperspectral data of the leaf, branch, and canopy level of the most commonly affected species will be collected, processed, and analyzed for discriminatory signatures of the disease in various stages of disease pathology. A controlled inoculation experiment will be conducted to provide the baseline spectral response in the absence of potentially disease-masking environmental factors such as drought, and other pathogens. Data obtained from the inoculation experiment and from the field will lead to the development of classification methods that can be applied to hyperspectral imagery that will be obtained over the study area in a scheduled acquisition from the Hyperion satellite. The ultimate goal of this research is to determine the feasibility of early disease detection through the application of hyperspectral technology.

Introduction

Remote sensing plays a pivotal role in the characterization of important ecological and environmental variables from local to global scale. The ability to monitor and track changes in nutrient, carbon, and water cycles, land use and land cover, forest structure and function, habitat, and invasive species is critical to the understanding of ecosystem and climate models (Kerr and Ostrovsky, 2003). Remote sensing platforms such as Landsat have made great contributions to environmental research over the past three decades. However, as environmental scientists probe ever deeper into ecosystem processes and models, the importance and need of higher spatial, spectral, and temporal resolutions for our orbital and airborne sensors has become apparent (Wulder, et al. 2004). The development of high spectral resolution (Hyperspectral) image sensor technology (Hyperion, AVIRIS, HyMap) in the mid-1990's has revolutionized both environmental and geologic analysis of the earth's surface for its ability to discriminate subtle spectral signatures of mineralogy, soil moisture, vegetation type, and vegetation stress (van der Meer, 1998; Kruse, Boardman, Huntington, 2003; Mumby, et al., 2004; Schmidt and Skidmore, 2003; Apan, et al. 2004). Hyperspectral remote sensing and field-based spectrometry, employed in concert, offer significant opportunities to delineate and discriminate particular environmental variables – variables previously considered difficult, if not impossible, to isolate using existing multispectral, broadband imagery. The goal of this research project is to develop and conduct an environmental investigation of the pathogenesis of oak wilt disease in the woodlands of central Texas using field-spectrometry and analysis of hyperspectral imagery. In the course of searching for the discriminating signature of oak wilt-induced physiological stress on afflicted oak species, I will be collecting and cataloging significant data on the general spectral signatures of these species as they progress through their phenological cycles in a variety of environmental settings. The spectral libraries that will be built of central Texas woodland species will begin to fill a much-needed data gap in vegetation spectral information. Building a spectral library, however, is only the groundwork for the spectral analysis needed to adequately assess and classify hyperspectral data. The spectra of vegetation materials must be statistically separable; if not, then little possibility exists that the endmembers they represent will be spectrally distinct in the hyperspectral imagery (Herold, M., et al., 2004).

Background of Oak Wilt

Disease pathogens such as Dutch Elm Disease and Chestnut Blight have wreaked havoc on North American forests during the 20th century. A less virulent pathogen, but potentially as devastating in its impact, is the pathogen responsible for the destructive vascular disease in *Quercus* spp., the fungus *Ceratocystis fagacearum* (Wilson, A. D., 2001). Commonly known as oak wilt, this disease claims many thousands of trees annually from the upper midwest to central Texas, resulting in significant property, ecological, and aesthetic losses (Appell, D. N., 1995). Multispectral and high spatial resolution remote sensing have been shown to be effective in identifying oak wilt mortality centers but only in middle to late stages of disease pathology - stages of defoliation and/or leaf discoloration (Everitt, J. H., Escobar, D. E., 1999). Of particular importance in disease management is the ability to detect disease centers in their earliest stages of development. My approach, using in-situ hyperspectral technology, is to

construct a spectral library of the pathology of oak wilt in the most commonly affected oak species native to central Texas. Filtered by a spectral baseline of healthy trees as they progress through their phenological stages, my goal is to look for a hyperspectral signature of the disease, data that will ultimately be convolved to airborne and satellite hyperspectral sensors, such as Hyperion and AVIRIS. Success in this project has ramifications for early detection of numerous forestry pathogens, invasive species, and disease vectors.

Literature review

A significant component of my data analysis will be to find and evaluate statistical methods for determining the spectral separability of individual species as well as the spectral separability of signatures of tree stresses. One such method, from a study of spectral discrimination of urban area materials – such as road surface types, roofing material types – was conducted by Herold, et. al. (2004). Spectral properties of these materials were field collected with a FieldSpec Pro spectroradiometer over the spectral range of 350 – 2400 nm. 147 individual target materials were sampled yielding over 5500 individual spectra. A data analysis technique known as the Bhattacharyya distance or B-distance was utilized to assess spectral separability. This B-distance is defined as (Eq. (1)):

$$B = \frac{1}{8} [\mu_1 - \mu_2]^T \left[\frac{\Sigma_1 + \Sigma_2}{2} \right]^{-1} [\mu_1 - \mu_2] + \frac{1}{2} \ln \frac{\left| \frac{1}{2} [\Sigma_1 + \Sigma_2] \right|}{\sqrt{|\Sigma_1| |\Sigma_2|}} \quad (1)$$

where μ_i and Σ_i are the mean vector and the covariance matrix of class one and two, respectively. This technique, developed to measure the statistical distance between two Gaussian distributions, also shows promise for the investigation of the most suitable bands for materials (urban or vegetation) classification.

Some authors have questioned whether - due to the spectral variation within species - it is possible to define a representative spectral profile for a species (Cochrane, M., 2000). Cochrane, in his study of the spectral variability within mahogany species of the Brazilian Amazon, cites numerous studies that have pointed out that intraspecies variance can occur due to variability in soils, climate, precipitation, and topography in addition to stress factors such as drought, disease, and pollution. Phenologic age and even leaf position in the canopy have been shown to explain substantial difference in the spectral signatures of some species. The first two metrics that Cochrane used to quantify relative spectral similarity between species were a root mean square difference (Eq. (2)) between a spectra and a standard and a vector angle difference between the same spectra that indicated variation in spectral shape (Eq. (3)).

$$D = \left[\frac{1}{N-1} \sum_{i=1}^N [S_M(\lambda) - S_a(\lambda)]^2 \right]^{1/2} \quad (2)$$

Where S_m and S_a are the standard and test spectra respectively, and N = number of spectral intervals.

$$\theta = \cos^{-1} \left[\frac{\int S_M(\lambda) S_a(\lambda) d\lambda}{\left[\int S_M(\lambda)^2 d\lambda \right]^{1/2} \left[\int S_a(\lambda)^2 d\lambda \right]^{1/2}} \right] \quad (3)$$

Where S_m and S_a again correspond to the standard and test spectra (which are normalized to remove amplitude dependence).

A third method he used for relative spectral discrimination was an analysis of variation of red-edge reflectance (from 680 – 730 nm). From a calculation of the red-edge first derivative, Cochrane determined the maximum inflection magnitude, the wave band where it occurred, and the four statistical moments (mean, variance, skewness, and kurtosis). These data indicated, at least for the species under consideration, good potential for separability. Finally, for the purposes of a classification scheme, Cochrane developed a new technique utilizing shape filtering. This filtering is based on the shape space for each species (at the branch and tree scale level) and is calculated (Eq. (4)) from the minimum and maximum reflectance values for each waveband, normalized to the species standard (the species average spectral profile).

$$S_{Na}(\lambda) = \frac{S_a(\lambda)}{S_M(\lambda)} \quad (4)$$

An example of the shape space of mahogany trees ($n = 25$) and of two species that are enveloped within that shape space and are thus spectrally indistinguishable can be seen in Figure 1. This spectral shape filtering technique can be used as well to determine the most optimum bands or subset of bands for spectral discrimination of species. It could also be custom modified to include the temporal or phenologic variation within a species. A species that is not spectrally separable at a particular “snapshot” time might be separable through filtering in spectral shape-time domain.

Other techniques for assessing the most optimal subset of hyperspectral wavebands for vegetation analysis applications was examined in two papers by Thenkabail, P.S., et al. (2004). This study of the spectral discrimination of tree, shrub, and weed species in a tropical forest habitat utilized several methods for determining the least redundant set of wavebands – principal component analysis, lambda-by-lambda R^2 contour plots, and stepwise discriminant analysis. The lambda-by-lambda method computes the coefficient of determination (R^2) for each and every combination of wavebands for all vegetation spectra. All R^2 values are then loaded into an $n \times n$ ($n =$ number of wavebands) matrix and contoured according to the lowest values of R^2 – values that reflect the least correlated pairs of wavebands. The optimal waveband information from all three methods yielded similar results. These papers of Thenkabail merit continued study and analysis for application to my research goals.

An informative paper by Pu, R., et al., (2003) investigated the correlation between spectral absorption features in oak leaves and corresponding relative water content (RWC, %) of oak leaves of species affected by the Sudden Oak Death epidemic in California. The author’s premise was that the leaves of infected trees had a different water status from those of healthy trees prior to the onset of visible symptoms such as leaf browning. This idea is essentially the premise of my investigation, that there could

exist a water stress signal in the spectra of oak-wilt infected trees prior to visible manifestations of the disease. The authors of this paper analyzed 139 reflectance spectra, particularly between wavebands 900 and 1300, for such absorption trough features (continuum removed) as trough depth, width, area, and wavelength at maximum depth. Although the results indicated moderately good correlation coefficients (R values) across the sampled range of RWC (10 – 60 %), 0.81 to 0.86 for depth and area features at absorption troughs 920 – 1120 nm and 1070 – 1320 nm, the data for the RWC range of 40 – 60%, corresponding to the green leaves of both infected and healthy trees, indicated little correlation and large deviation from the regression line. Their work, while potentially useful, yielded little support for their premise that infected trees can be spectrally discriminated from healthy trees based on the RWC of visibly healthy, still green leaves. However, I'm confident that I can improve on their methodology through a more thorough analysis of the spectra, including the red-edge response to water stress.

Other papers await examination for their contributions to the hyperspectral discrimination of both vegetation species and disease-induced stress factors. Australian sugar-cane varieties and their subseptibility to orange rust fungal disease have been successfully discriminated through multiple discriminant analysis and vegetation indices (Galvao, et al., 2005). A study of plant stress associated with below-ground natural gas leaks and subsequent soil oxygen depletion demonstrated that first derivative analysis of the red-edge and derivative peak ratios indicated statistically significant stress signals 7 days prior to any visible symptoms (Smith, K. L., et al., 2004).

Experimental Design

This research project will be based on the collection, processing, and analysis of data from 3 primary sources – field data from known oak wilt mortality centers, a controlled greenhouse experiment, and hyperspectral satellite imagery scheduled for a June acquisition. The experimental design of any field investigation of the environment is crucial to the integrity of the data collected and ultimately the success of the project. With a field investigation of the spectral properties of vegetation, there are a number of additional concerns unique to spectrometry. In a general sense, being aware of and planning for such issues as viewing and illumination geometry, atmospheric characteristics, wind, timing of the data collection, and the collection of ancillary data sets and metadata, is fundamental to any successful field campaign (Zomer, R. et al., <http://cstars.ucdavis.edu/classes/hsgrdtutorial.html>). Other experimental design concerns become apparent depending on the specific question or problem to be addressed. For this particular study of the spectral signature of oak wilt pathogenesis I will have to customize the experimental design in such a way to minimize other abiotic and biotic variables – variables such as drought stress, geographic location, tree age, competition, phenology, and other pathogens. The optimum approach then is to collect spectral data affected by as few external variables as possible. A recent decision to conduct a controlled greenhouse experiment contemporaneous with initial field data collection will enable me to minimize many of the environmental variables capable of masking an oak wilt stress signal. This greenhouse study will be a *Ceratocystis fagacearum* inoculation experiment using twenty *Quercus fusiformis* (live oak) saplings, container grown in 5 gallon pots. Specimens will be obtained from a local wholesale nursery and are guaranteed to be

grown from local seed stock. This experiment will be a 2 factor, crossed design (inoculated – water stressed, inoculated – not water stressed, not inoculated – water stressed, and not inoculated – not water stressed) with 5 or more replications. Arrangements have been made to acquire *Ceratocystis fagacearum* inoculum from the plant pathology laboratories at Texas A&M. Inoculum will be cultured and preserved for future use in the laboratory of Dr. Adria Bodour. Dependent variables to be assessed will be spectral response at the leaf level, leaf relative water content, leaf fluorescence, and photosynthetic activity. Data will be collected on a 7 - 10 day cycle for a 6 month period (or until tree mortality by a confirmed oak wilt infection). Spectral data will be analyzed for statistically significant signals of stress due to a successful infection. The success of the field data campaign will largely depend on the information gathered and the results obtained in the controlled experiment.

The following represents a preliminary experimental design and data collection protocol for my field campaign.

1. Data collection time – at or near solar noon, plus or minus 2 hours
2. Data collection intervals – weekly or bimonthly
3. Experimental data collection sites – two recently identified (within 3 years) oak wilt mortality centers will serve as study sites. These study sites will be located within the proposed Hyperion acquisition area (see Figure 1). Two additional oak wilt sites, one at the Kerrville Forest Service property and another at the Hill Country State Natural Area in Bandera County, will also be surveyed. Mortality centers where disease mitigation such as fungicide application, tree removal, or bulldozing will disqualify that site from the study. A mortality center that has been trenched, however, will be considered given that sufficient distance exists from the “dead zone” to the trench to allow for a sufficient sample size of living trees.
4. Control data collection sites – specific sites/trees (in supposed good health) will be randomly selected for control both within and outside the Hyperion image acquisition area. Efforts will be made to select trees in locations with similar environmental conditions to those of the experimental trees.
5. Sampling design – individual trees of similar size and age (determined by bole size at 4’ above ground level) will be leaf, branch, and canopy sampled. The branch and canopy (where possible) samples will be taken with the spectrometer probe at nadir position. Efforts will be made to select trees in a random design; all selected trees will be geolocated to within 1 meter with differential GPS. Individual leaves will be sampled at both random and fixed (eg. specific leaves) locations on the tree – drip edge, canopy, and interior. Ancillary data such as estimated tree height, bole size, crown spread, distance to centroid of dead zone, and distance to nearest neighbors will be collected, as well as site, light, and weather conditions.

Field Sampling

I have begun collecting spectral radiance data at the individual leaf level of the following species known to be afflicted with the oak wilt fungus (Appell, D. N., 1984).

- Spanish Oak (*Quercus texana*)
- Live Oak (*Quercus fusiformis* and *Quercus virginiana*)
- Post Oak (*Quercus stellata*)
- Blackjack Oak (*Quercus marilandica*)

Baseline spectra of the following common central Texas woodland species will also be collected and analyzed for a future spectral library.

- Honey Mesquite (*Prosopis glandulosa*)
- Cedar Elm (*Ulmus crassifolia*)
- Juniper (*Juniperus ashei*)
- Sycamore (*Platanus occidentalis*)
- Cottonwood (*Populus deltoides*)

Methods

All trees that have been sampled to date have been geolocated with GPS. Over 30 individual trees have been sampled and more than 200 leaf radiance spectra collected. Generally at least 5 leaf specimens are taken from each tree. To acquire foliage samples, individual leaves are clipped from trees at varying locations close to branch tips, immediately cataloged, and stored in ziplock bags to mitigate any dessication effects. Generally within 30 minutes, radiance data are collected from each leaf using an Analytical Spectral Devices (ASD) FieldSpec Pro spectroradiometer. This instrument records in 2150 wavebands over the range of 350 – 2500 nm, with an interpolated resolution of 1 nm. Prior to each sampling, the instrument is optimized for dark current levels, and then calibrated against a Labsphere Spectralon white reference panel. White reference radiance is collected and saved to the first file in a sampling run. Each file consists of 10 consecutive radiance spectra collected over a period of 3 seconds, averaged to reduce ambient noise. All leaf samples are placed individually on a painted flat-black panel to minimize reflection, and illuminated from an ASD xenon light source leaf probe, in direct contact with the leaf.

Individual leaves are sampled on the top or adaxial surface, generally one spectra collected per leaf. However, some larger leaves are sampled at 2 or 3 locations across the leaf surface. Occasionally, spectra are collected on the back or abaxial surface for comparison. In addition to individual leaf spectra, I have also collected spectra on stacks of leaves to evaluate the effects of additive reflectance. One spectra for the first leaf is collected, then a spectra for a stack of two, then a stack of three, etc. In most cases, I have stacked at least 5 leaves for analysis. So as to not bias the results by the topmost leaf in the stack, I randomly create new stacks from a larger set of leaves.

Spectral radiance data are collected directly on the laptop PC that runs the ASD software. Files are in binary format and are named according to tree type, date, and a GPS waypoint number. The file qf_40505_3 designates a radiance file collected on April 5, 2005 on a *Quercus fusiformis* (live oak) at waypoint 3. All GPS location information is kept in an Excel spreadsheet. I have the option of converting all binary files to ASCII text files. Ultimately, I will routinely convert all files as the ASCII format will be easier to process in an Excel or IDL batch mode. Future work will consist of developing batch routines for the conversion of radiance data to reflectance, as well as for statistical processing and analysis.

The first step in processing the spectral file is to convert the radiance values to target reflectance, where the target reflectance is the ratio of energy reflected off the target (e.g., leaves) to energy incident on the target (measured using the Spectralon white reference). Files are processed using the ENVI program using the following routines:

- 1) spectral library builder – reads the ASD binary formatted files and builds an ENVI formatted spectral library file or output ASCII file
- 2) spectral library viewer – displays plots of files within a spectral library
- 3) spectral math – converts radiance target and reference spectral library files to reflectance using the following equation.

$$\text{Reflectance} = \text{radiance}_{\text{target leaf}} / \text{radiance}_{\text{white reference}}$$

Preliminary results and discussion

The mean (+/- 1 standard deviation) reflectance spectra of 54 leaves from nine individual *Q. fusiformis* sampled over a 2 week period from April 6 – 20 can be seen in Figure 2. The degree of variance is not surprising considering the changes taking place in the newly emergent leaves, such as onset of photosynthesis, varying water, cellulose, and lignin content. As the leaves harden off and mature and other environmental factors come into play as the growing season progresses, it will be interesting to compare the spectral changes. Although based on just single samples, an example of these environmental and phenological changes can be seen in the comparison between a leaf spectra acquired in mid February, representing a late season state just before leaf drop, and one taken from the same tree in early April, representing a new emergent leaf (Figure 3). Some of the spectral variation could be explained by statistical variance, yet certain features emerge that I think are clear indications of physical/temporal changes. The reduction and the red shift in the green peak at 550 - 560 nm corresponds to changes in pigmentation chemistry (loss of chlorophylls and gain of carotenoids). The increase in reflectance and the changes in slope of the near infrared, 750 – 1300 nm, are probably due to changes in mesophyll layer water content and structure. A complete phenological cycle of spectral changes will ultimately be acquired and may provide clues to classification algorithms for species discrimination.

The phenomena of additive reflectance may also yield valuable information for the discrimination of species at the canopy level and for the detection of oak wilt-induced stress. As the leaf area index (LAI) increases for a particular tree, the effects on the overall reflectance in the NIR are profound. This phenomena can be replicated at the leaf level by taking successive radiance measures (then converting to reflectance) of

incrementally stacked leaves. An experiment was conducted with 28 *Q. fusiformis* leaves collected from 6 different trees on my property. Reflectances were acquired for all 28 individual leaves, followed by reflectances for 15 randomly selected stacks of two, followed by 12 random stacks of 3, etc. I finished with 5 random stacks of 6, expecting complete spectral saturation of the NIR at that level. Each group of spectra for each stack was averaged, and the averaged spectra were plotted together (Figure 4). It is immediately apparent that saturation occurs with a single leaf in the visible region (400 – 700 nm), and perhaps with 2 leaves in the short wave infrared (1300 – 2500nm). However, saturation for *Q. fusiformis* leaves for the NIR, at this point in the growing season, is probably at 7 – 8 leaves. The progressive increase in slope is one intriguing aspect of the spectral behavior in the 760 – 920 nm region of the NIR, an aspect that deserves much more analysis. The results of this experiment indicate several exciting possibilities; the first being that a better predictive model for canopy leaf density or LAI could be built, second that these results could suggest new vegetation indices or classification algorithms specific to species and/or stress discrimination.

Leaf water stress should be a key indicator of an oak wilt infection as the primary pathology of the disease involves a fungal invasion of water-conducting vessels in the xylem which trigger the formation of tyloses which plug the vessels. Therefore knowledge of the spectral changes that occur as a leaf undergoes progressive water loss could also yield important information for this study. A simple experiment was designed to test the effects of leaf drying, or water loss, on a cedar elm leaf (*Ulmus crassifolia*) by setting up the spectroradiometer to collect a data sample every 3 minutes for one hour while the leaf probe was in continuous contact with the leaf. The heat from the leaf probe lamp provided the drying mechanism. It is recognized that this experiment does not replicate natural conditions – the drying rate was greatly accelerated and the high heat and light intensity of the probe probably induced chemical changes in the leaf pigments that would not occur in nature. However, the results are interesting and worthy of further study – especially, if the degree of water loss is quantified by making successive weighings. The trend of spectral profile changes as the *U. crassifolia* leaf dried are portrayed in Figure 5.

Conclusions

The work completed so far represents a fraction of the quantity of data and degree of analysis that will be necessary to answer the fundamental question posed by this research. As with most investigations, new questions present themselves faster than answers are found. Hyperspectral technology is on the cutting edge of remote sensing – only with thorough investigations of its potential can the fundamental questions be answered.

References cited

Apan, A., Held, A., Phinn, S., (2004). Detecting sugarcane 'orange rust' disease using EO-1 Hyperion hyperspectral imagery. *International Journal of Remote Sensing*, 25, 489 – 498.

Appell, D. N., (1984). Aerial survey for oak wilt incidence at three locations in central Texas. *Plant Disease*, 68, 661 – 664.

Appell, D. N., (1995). The oak wilt enigma – Perspective from the Texas epidemic. *Annual Review of Phytopathology*, 33, 103 – 118.

Cochrane, M. A., (2000), Species classification using vegetation reflectance variability. *International Journal of Remote Sensing*, 21, 2075 – 2087.

Everitt, J. H., Escobar, D. E., (1999). Using airborne digital imagery for detecting oak wilt disease. *Plant Science*, 83, 502 – 505.

Galvao, L. S., Formaggio, A. R., Tisot, D. A. (2005). Discrimination of sugarcane varieties in Southeastern Brazil with EO-1 Hyperion data. *Remote Sensing of Environment*, 94, 523– 534.

Herold, M., Roberts, D. A., Gardener, M. E., Dennison, P. E., (2004). Spectrometry for urban area remote sensing – Development and analysis of a spectral library from 350 nm to 2400 nm. *Remote Sensing of the Environment*, 91, 304 – 319.

Kerr, J. T., Ostrovsky, M. (2003). From space to species: Ecological applications for remote sensing. *Trends in Ecology and Evolution*, 18, 299 – 314.

Kruse, F. A., Boardman, J. W., Huntington, J. F. (2003). Comparison of airborne hyperspectral data and EO-1 Hyperion for mineral mapping. *IEEE Transactions on Geoscience and Remote Sensing*, 41, 1388-1400.

Mumby, P. J., Skirving, W., Strong, A. E., Hardy, J. T., LeDrew, E. F., Hochberg, E. J., Stumpf, R. P., David, L. T. (2004). Remote sensing of coral reefs and their physical environment. *Marine Pollution Bulletin*, 48, 219 – 228.

Pu, R., Ge, S., Kelly, N. M., Gong, P., (2003). Spectral absorption features as indicators of water status in coast live oak (*Quercus agrifolia*) leaves. *International Journal of Remote Sensing*, 24, 1799 – 1810.

Schmidt, K. S., Skidmore, A. K. (2003). Spectral discrimination of **vegetation** types in a coastal wetland. *Remote Sensing of the Environment*, 85, 92-108

Smith, K. L., Steven, M. D., Colls, J. J. (2004). Use of hyperspectral derivative ratios in the red-edge region to identify plant stress responses to gas leaks. *Remote Sensing of the Environment*, 92, 207 – 217.

Van der Meer, F. (1998). Imaging spectrometry for geological remote sensing. *Geologie En Mijnbouw*, 77, 137+.

Wilson, A. D., (2001). Oak wilt – A potential threat to southern and western oak forests. *Journal of Forestry*, 99, 4 – 11.

Wulder, M. A., Hall, Ronald, R. J., Coops, N. C., Franklin, S. E., (2004). High spatial resolution remotely sensed data for ecosystem characterization. *BioScience*, 54, 511 – 521.

Zomer R. and Ustin S. Ground-Truth Data Collection Protocol For Hyperspectral Remote Sensing, University of California Davis.
<http://cstars.ucdavis.edu/classes/hsgrdtutorial.html>

List of Figures

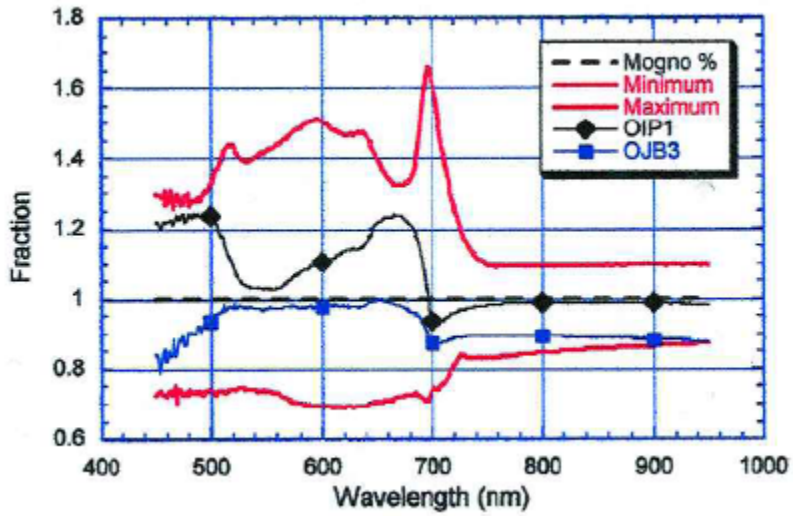


Figure 1. A spectral space shape filter for Mahogany.

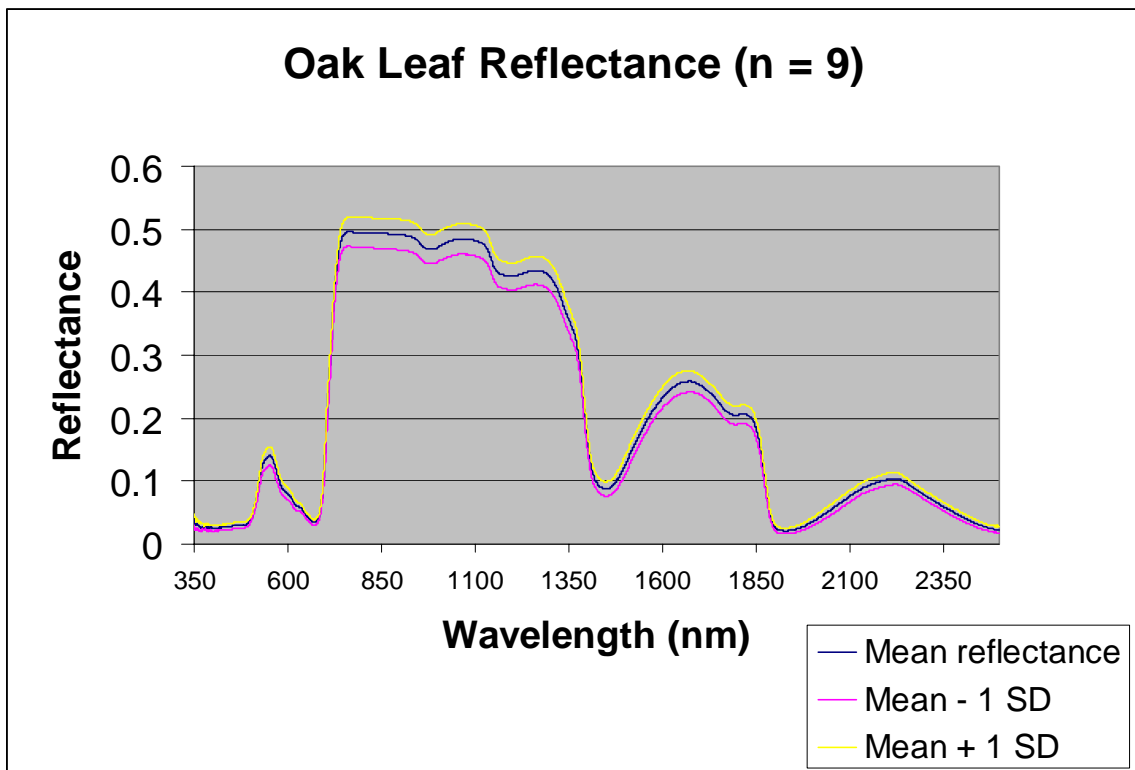


Figure 2. Spectral variability of *Q. fusiformis* leaves.

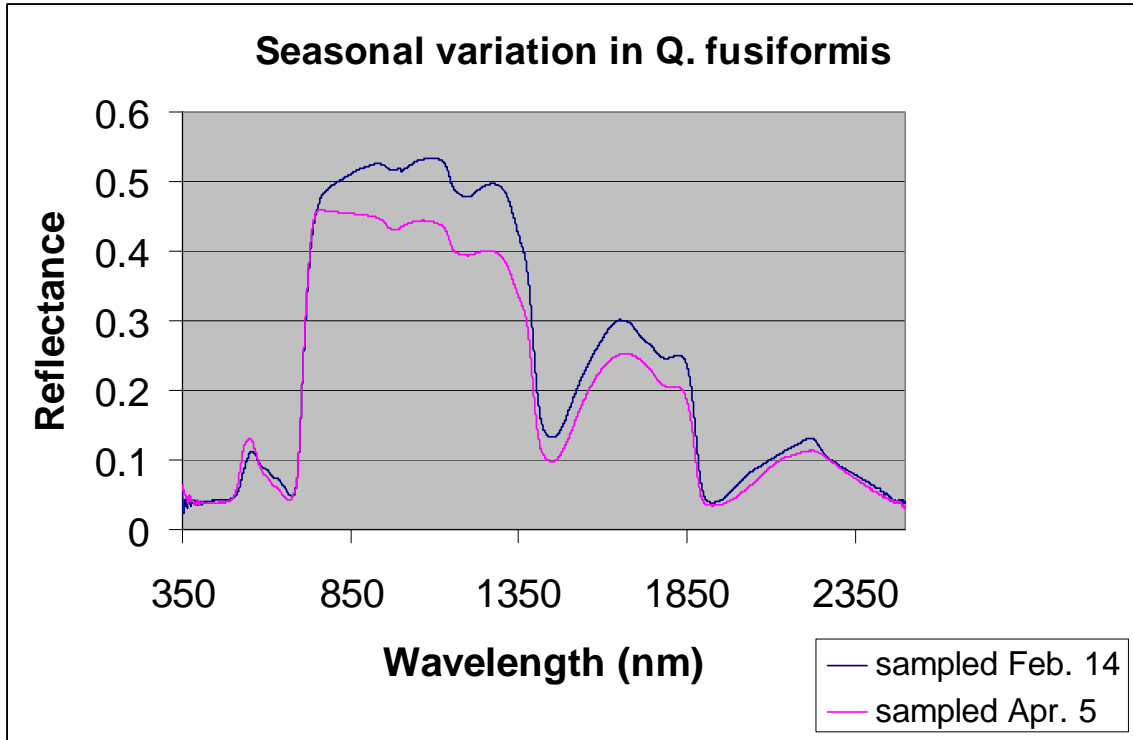


Figure 3. A Seasonal variation in *Q. fusiformis*

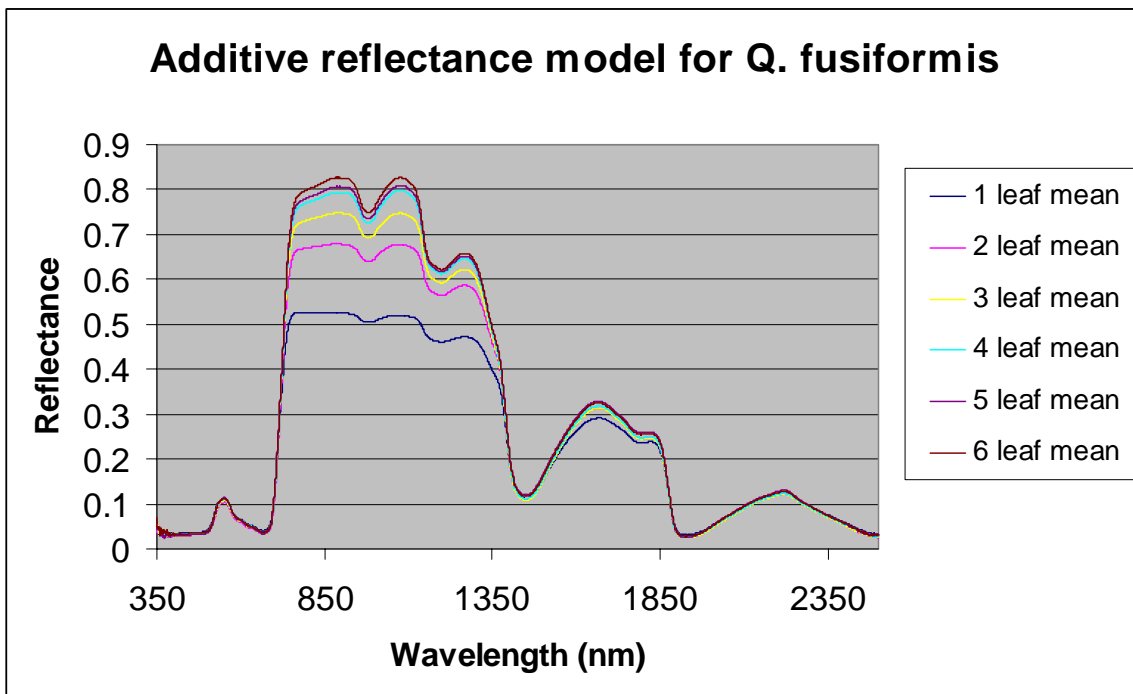


Figure 4. Additive reflectance model for *Q. fusiformis*

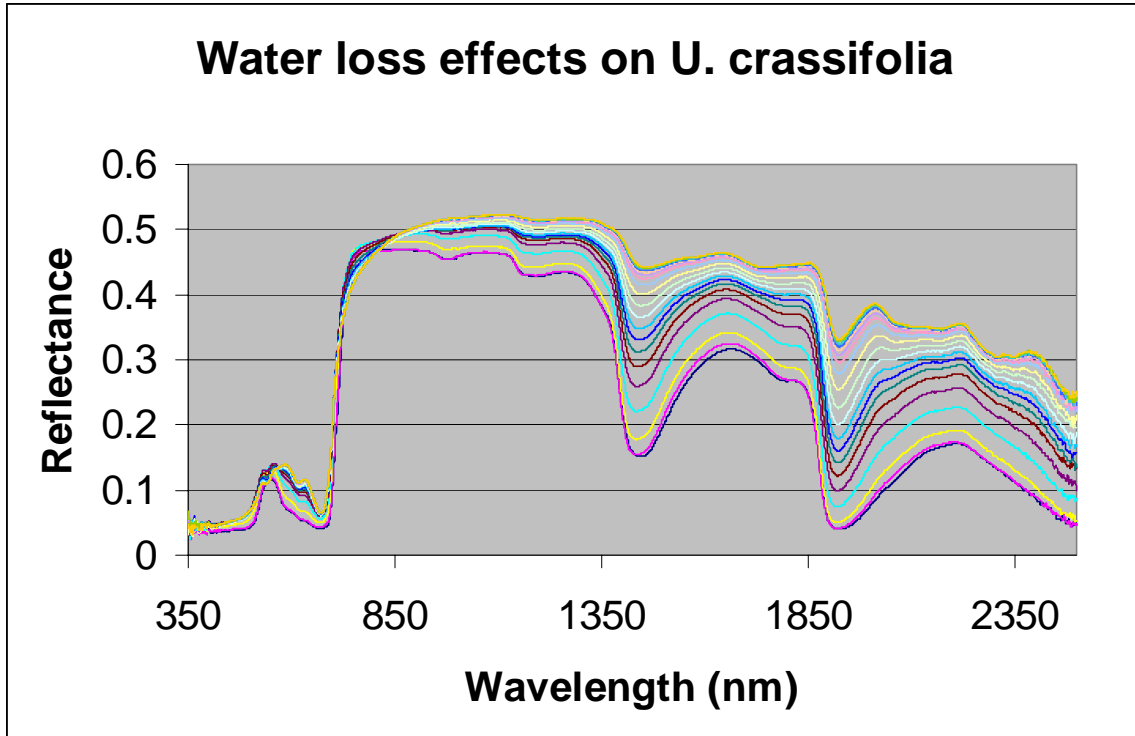


Figure 5. Spectral profiles of water loss effects on *U. crassifolia*